Japanese Journal of
Applied Physics

Numerical Simulation of Laser Induced Weakly Ionized Helium Plasma Process by Lattice Boltzmann Method

To cite this article: Xiaobo Zhang *et al* 2012 *Jpn. J. Appl. Phys.* **51** 01AA04

Japanese Journal of Applied Physics **51** (2012) 01AA04 **REGULAR PAPER**
DOI: 10.1143/JJAP.51.01AA04

Numerical Simulation of Laser Induced Weakly Ionized Helium Plasma Process by Lattice Boltzmann Method

Xiaobo Zhang[1,2], Yoshihiro Deguchi[2*], and Jiping Liu[1]

[1] *School of Energy and Power Engineering, Xi'an Jiaotong University, Xi'an 710049, China*
[2] *Department of Mechanical Engineering, The University of Tokushima, Tokushima 770-8501, Japan*

Received May 3, 2011; revised September 20, 2011; accepted September 30, 2011; published online January 20, 2012

Generation process of laser induced weakly ionized helium plasma is simulated using the lattice Boltzmann method (LBM). Maxwell equations, which are used to model the propagation of laser, are calculated by the finite difference time domain (FDTD) method. Employing coefficients of distribution functions, processes of multi-photon ionization, electron impact ionization and three-body recombination are included in Boltzmann equations. Using *D2Q9* model in LBM, number densities of particles in plasma can be obtained after solving Boltzmann equations. For the energy transformation in plasma, the finite volume method (FVM) is applied to calculate the macroscopic energy equations directly coming from the continuous Boltzmann equations. Interaction between laser and plasma as well as laser induced weakly ionized plasma are demonstrate to validate the hybrid model.

1. Introduction

Laser induced plasma (LIP) is an essential and important process in many laser applications such as laser induced breakdown spectroscopy (LIBS), laser ignition, laser welding and nuclear fusion. However LIP exhibits very complex and transient phenomena, measuring devices are not enough rapid and precise to track the all minor changes, then numerical simulation is becoming a primary method to reveal the essence of LIP.

Currently, macroscopic methods based on hydrodynamics and microscopic methods depending on molecular dynamics are the most popular ways for LIP simulation. In macroscopic methods, movements and energy transformation of particles in plasma are modeled by Navier-Stokes equations based on continuum hypothesis. The mature numerical methods in hydrodynamics, such as finite volume and finite difference, are used to solve those equations. The shortcoming of these methods is that it is difficult to add related microscopic processes into hydrodynamic equations. Particle in cell (PIC) is the most used microscopic method,[1)] an equation is utilized for the evolution of each particle in plasma. Theoretically all physical processes can be retained in the equation, but the high computational expense even for small physical domain limits use of PIC.

In recent decades, lattice Boltzmann method (LBM) has the great development and has been successfully used for fluid simulations. As a mesoscopic method, LBM has many advantages for micro-channel and porous flow simulation.[2)] As known, evolution of particles as well as deeper microscopic processes in plasma can be modeled using Boltzmann equation, so models in LBM have the potential to be used for plasma simulation. Comparing to PIC, the physical region modeled by LBM can be larger and the computational cost is not very high.

However, when physical parameters of particles in plasma are directly used, lattice Boltzmann equation becomes a collisionless equation because of too large dimensionless relaxation time, and then all simulation is just the migration process of particles. To overcome this problem, in the paper of Li,[3)] a rescaling process is adopted before simulation, then an electron diffusion problem under electrostatic field is used to validate this method. In addition, considering electron impact ionization, three-body recombination as well as energy conservation and transformation processes, interaction between laser and weakly ionized helium has been successfully simulated using LBM.[4)] In the present paper, the whole generation and development processes of laser induced weakly ionized helium plasma are considered, and the microscopic processes contain multi-photon ionization, electron impact ionization and three-body recombination. Besides, laser's focusing process and the plasma growth process according to laser energy absorption are also considered.

2. Mathematic Models

2.1 Propagation of laser

Here laser is simplified as a Gaussian beam, and its propagation is modeled using Maxwell equations:

$$\nabla \times \mathbf{H} = \varepsilon \frac{\partial \mathbf{E}}{\partial t} + \mathbf{J}, \tag{1}$$

$$\nabla \times \mathbf{E} = -\mu \frac{\partial \mathbf{H}}{\partial t}. \tag{2}$$

In the above equations, $\mathbf{H}$ and $\mathbf{E}$ are magnetic and electric field respectively, ε and μ are permittivity and magnetic permeability, and $\mathbf{J}$ is the current density by movements of electrons and ions in plasma. In order to get Gaussian beam's electromagnetic field in real time, the finite difference time domain (FDTD) method is used to solve the above equations. Besides, the perfectly matched layer absorbing boundary condition is adopted outside the computational region to prevent the boundary reflection of electromagnetic waves in FDTD.[5)]

2.2 Generation and development of plasma

Assuming plasma as one kind of fluid and considering the accelerated processes of charged particles in the electromagnetic field of laser, evolution processes of electrons, ions and neutrals in plasma can be described using Boltzmann equations as follows:

$$\frac{\partial f_e}{\partial t} + \mathbf{v}_e \cdot \nabla f_e + \mathbf{a}_e \cdot \nabla_{\mathbf{v}_e} f_e = -\frac{f_e - f_{en}^{eq}}{\lambda_{en}} + R_e f_e^{eq}, \tag{3}$$

$$\frac{\partial f_i}{\partial t} + \mathbf{v}_i \cdot \nabla f_i + \mathbf{a}_i \cdot \nabla_{\mathbf{v}_i} f_i = -\frac{f_i - f_{in}^{eq}}{\lambda_{in}} + R_i f_i^{eq}, \tag{4}$$

*E-mail address: ydeguchi@me.tokushima-u.ac.jp

$$\frac{\partial f_n}{\partial t} + \mathbf{v}_n \cdot \nabla f_n = -\frac{f_n - f_{nn}^{eq}}{\lambda_{nn}} + R_n f_n^{eq}. \quad (5)$$

In eqs. (3)–(5), the subscripts s (e, i, or n) denote the type of particles and take e, i, or n for electrons, ions, or neutrals respectively. f_s is the distribution function, and f_s^{eq} is the distribution function in equilibrium state. $\mathbf{v}_s$ is the microscopic velocity of particle species s. $\mathbf{a}_s$, the acceleration of charged particles by the Lorentz force, can be calculated as $\mathbf{a}_s = q_s(\mathbf{E} + \mathbf{v}_s \times \mathbf{B})/m_s$, where q_s and m_s are the charge and mass of the particle. In this paper, only weakly ionized plasma is considered, so long-range Coulomb interaction between charged particles is ignored. In the interaction among particles in plasma, only binary collisions of electron–neutral, ion–neutral, and neutral–neutral are considered. λ_{en}, λ_{in}, and λ_{nn} are the relaxation times for electron–neutral, ion–neutral, and neutral–neutral collisions, and f_{en}^{eq}, f_{in}^{eq}, and f_{nn}^{eq} are the equilibrium distribution functions of electrons, ions and neutrals respectively due to their collisions with neutrals. R_s is the total coefficient of ionization and recombination of particle species s, and it contains R_s^{mpi} of multi-photon ionization, R_s^{eii} of electron impact ionization, and R_s^{tbr} of three-body recombination.

For the acceleration terms in Boltzmann equations, several researchers propose simplified models. Here He's model is used,[6]

$$\mathbf{a}_s \cdot \nabla_{\mathbf{v}_s} f_s = -\frac{\mathbf{a}_s \cdot (\mathbf{v}_s - \mathbf{u}_s)}{\theta_s} f_s^{eq}. \quad (6)$$

$\mathbf{u}_s$ is the macroscopic velocity, and $\theta_s = \sqrt{k_B T_s/m_s}$ is the sound speed of particle species s where k_B is the Boltzmann constant.

According to gas kinetic theory,[7] the relaxation time of binary collisions can be calculated as: $\lambda_{sn} = 1/(\sigma_{sn} n_n \langle v_s \rangle)$, where $\sigma_{sn} = \pi(r_s + r_n)^2$ is the cross section of collisions between particle species s and neutrals, r_s and r_n are the radius of particle species s and neutrals. n_n is the number density of neutrals, and $\langle v_s \rangle = [(8/\pi)(k_B T/m_s)]^{1/2}$ is the average thermal speed of particle species s.[7]

The equilibrium distribution function of self-collision takes the following Maxwell-Boltzmann equation,

$$f_s^{eq} = \frac{n_s}{2\pi\theta_s^2} \exp\left[-\frac{(\mathbf{v}_s - \mathbf{u}_s)^2}{2\theta_s^2}\right]. \quad (7)$$

Similarly, the binary cross-collision equilibrium distribution function is

$$f_{sn}^{eq} = \frac{n_s}{2\pi\theta_{sn}^2} \exp\left[-\frac{(\mathbf{v}_s - \mathbf{u}_{sn})^2}{2\theta_{sn}^2}\right], \quad (8)$$

where $\mathbf{u}_{sn} = (\rho_s \mathbf{u}_s + \rho_n \mathbf{u}_n)/(\rho_s + \rho_n)$ is the barycentric velocity of binary collisions between particle species s and neutrals. The sound speed is defined as $\theta_{sn} = \sqrt{k_B T_{sn}/m_{sn}}$, where $m_{sn} = m_s m_n/(m_s + m_n)$ is the reduced mass of particle s and neutrals, and T_{sn} is temperature of particle species s after collision with neutrals in the time period of λ_{sn}. In eq. (5), only self-collisions have effect on the relaxation process of neutrals, so $f_{nn}^{eq} = f_n^{eq}$ is satisfied.

Depending on the collision theory in gas kinetics and considering processes of electron impact ionization and three-body recombination, T_{sn} has the following expressions:

$$T_{en} = T_e + \frac{2m_{en}(T_n - T_e)}{m_e + m_n} + \frac{m_n m_{en}(\mathbf{u}_n - \mathbf{u}_e)^2}{3k_B(m_e + m_n)} - \frac{2\lambda_{en}(R_e^{eii} - R_e^{tbr})U_i e}{3k_B}, \quad (9)$$

$$T_{in} = T_i + \frac{2m_{in}(T_n - T_i)}{m_i + m_n} + \frac{m_n m_{in}(\mathbf{u}_n - \mathbf{u}_i)^2}{3k_B(m_i + m_n)}. \quad (10)$$

In Boltzmann equations, the last term $R_s f_s^{eq}$ denotes changes of distribution functions of electrons, ions or neutrals due to ionization of neutrals and recombination of charged particles. When the photon number density in the laser field is enough large, electrons may get rid of the shackles of the nucleus because of multi-photon ionization. According to theory of Delone,[8] the ionization probability of neutrals in the laser-irradiated field can be calculated as

$$R_n^{mpi} = W I^N, \quad (11)$$

where W is the multi-photon ionization cross section, I is the laser intensity, and N is the minimum number of necessary photons for ionization of one neutral.[8] In this paper, only single ionization is considered, so coefficients of electrons and ions by multi-photon ionization have the following relations:

$$R_e^{mpi} = \frac{R_n^{mpi} n_n}{n_e}, \quad (12)$$

$$R_i^{mpi} = \frac{R_n^{mpi} n_n}{n_i}. \quad (13)$$

The electron impact ionization rate can be expressed as

$$R_e^{eii} = \sigma^{eii} n_n \langle v_e \rangle, \quad (14)$$

where σ^{eii} is electron impact ionization cross section. The data of σ^{eii} is dependent on the electron energy and can be found in the paper of Kim and Rudd.[9]

For the rate of three-body recombination, the formula in the paper of Kemp is adopted:[10]

$$R_e^{tbr} = \frac{0.822 \times 10^{-33}}{T_e^{4.5}} n_e n_i, \quad (15)$$

where T_e is temperature of electrons in the unit of eV.

Similarly with multi-photon ionization, R_i^{eii}, R_i^{tbr}, R_n^{eii}, and R_n^{tbr} can be calculated by $R_i^{eii} = R_e^{eii} n_e/n_i$, $R_i^{tbr} = R_e^{tbr} n_e/n_i$, $R_n^{eii} = R_e^{eii} n_e/n_n$, and $R_n^{tbr} = R_e^{tbr} n_e/n_n$ respectively. At last, the total coefficients of ionization and recombination are obtained as $R_e = R_e^{mpi} + R_e^{eii} - R_e^{tbr}$, $R_i = R_i^{mpi} + R_i^{eii} - R_i^{tbr}$, and $R_n = -R_n^{mpi} - R_n^{eii} + R_n^{tbr}$.

2.3 Energy conversion and transformation in plasma

There are complex energy conversion and transformation processes simultaneously existing in the interaction of laser and plasma. Under Lorentz force's act, electromagnetic energy of laser is conversed into charged particles' kinetic energy. At the same time of accelerated processes, charged particles have so frequent collisions with neutrals in their movements that their kinetic energy is conversed into internal energy. Besides, there are thermal conduction processes among particles in different temperature.

However, as a newly developed mesoscopic method, $D2Q9$ model in LBM cannot have a comprehensive description for such complex heat transfer process. In kinetic theory, if every term in the continuous Boltzmann

equations is multiplied by energy operator, macroscopic total energy equations can be obtained after integration process implemented in all velocity spaces.

Take electrons as an example, in eq. (3), multiplying $\chi(\mathbf{v}_e) = (1/2)m_e\mathbf{v}_e{}^2$ on each term and integrating the equation in the velocity space, the following equation is obtained:

$$\begin{aligned}\int_{\mathbf{v}_e}\chi(\mathbf{v}_e)\frac{\partial f_e}{\partial t}\,d\mathbf{v}_e + \int_{\mathbf{v}_e}\chi(\mathbf{v}_e)\mathbf{v}_e\cdot\nabla f_e\,d\mathbf{v}_e \\ = -\frac{1}{\lambda_{en}}\int_{\mathbf{v}_e}\chi(\mathbf{v}_e)(f_e - f_{en}^{eq})\,d\mathbf{v}_e + R_e\int_{\mathbf{v}_e}\chi(\mathbf{v}_e)f_e^{eq}\,d\mathbf{v}_e \\ + \frac{\mathbf{a}_e}{\theta_e^2}\int_{\mathbf{v}_e}\chi(\mathbf{v}_e)(\mathbf{v}_e - \mathbf{u}_e)f_e^{eq}\,d\mathbf{v}_e. \end{aligned} \tag{16}$$

Following similar derivation procedures in the book of Bittencourt,[11] the macroscopic energy equation of electrons is expressed as

$$\begin{aligned}&\frac{\partial\varepsilon_e}{\partial t} + \nabla\cdot(\varepsilon_e\mathbf{u}_e) \\ &\quad = -\nabla\cdot(\mathbf{P}_e\cdot\mathbf{u}_e) + \nabla\cdot(\mathcal{K}_e\nabla T_e) + \mathbf{J}_e\cdot\mathbf{E} \\ &\qquad - \frac{3k_B n_e m_{en}(T_e - T_n)}{\lambda_{en}(m_e + m_n)} + \frac{m_e n_e}{\lambda_{en}}\mathbf{u}_{en}\cdot(\mathbf{u}_{en} - \mathbf{u}_e) \\ &\qquad - (R_e^{eii} - R_e^{tbr})n_e Ue + R_e\varepsilon_e, \end{aligned} \tag{17}$$

where ε_e is the total energy of electrons. The first term on the right side is the acting of pressure to electrons' movements. The second term is the heat conduction between electrons and $\mathcal{K}_e = (1/2)n_e k_B\langle v_e\rangle l_e$ (l_e is the mean free path of electrons) is the thermal conductivity of electrons. $\mathbf{J}_e\cdot\mathbf{E}$ is the heated term of electrons by laser. In this term there is only electric field because magnetic field can only change movement directions of electrons. The fourth and fifth terms are energy exchange between electrons and neutrals in collisions. Considering that the transition existing in ionization and recombination is only between the ground and contious states, the sixth term denotes energy assumption in the processes of electron impact ionization and three-body recombination, and Ue is the first ionization potential of helium. The needed energy in multi-photon ionization comes from laser, so change rates in this term only contain R_e^{eii} and R_e^{tbr}. The last term represents total energy change of electrons due to variation of electron number density by multi-photon ionization, electron impact ionization and three-body recombination. Using the number density and velocity from LBM, eq. (17) is solved by the finite volume method.

Ions and neutrals' energy equations can be derived in a similar way. However, in electron impact ionization, the ionization potential of neutrals is only supplied by electrons, and electrons get the released energy in the process of three-body recombination. Therefore it is not necessary to consider the energy change because of electron impact ionization and three-body recombination in ions' energy equation. For neutrals, because Lorentz force can only act on charged particles, there is no joule heating term in their energy equations:

$$\begin{aligned}\frac{\partial\varepsilon_i}{\partial t} + \nabla\cdot(\varepsilon_i\mathbf{u}_i) &= -\nabla\cdot(\mathbf{P}_i\cdot\mathbf{u}_i) + \nabla\cdot(\mathcal{K}_i\nabla T_i) \\ &\quad + \mathbf{J}_i\cdot\mathbf{E} - \frac{3k_B n_i m_{in}(T_i - T_n)}{\lambda_{in}(m_i + m_n)} \\ &\quad + \frac{m_i n_i}{\lambda_{in}}\mathbf{u}_{in}\cdot(\mathbf{u}_{in} - \mathbf{u}_i) + R_i\varepsilon_i, \end{aligned} \tag{18}$$

$$\begin{aligned}&\frac{\partial\varepsilon_n}{\partial t} + \nabla\cdot(\varepsilon_n\mathbf{u}_n) \\ &\quad = -\nabla\cdot(\mathbf{P}_n\cdot\mathbf{u}_n) + \nabla\cdot(\mathcal{K}_n\nabla T_n) \\ &\qquad + \frac{3k_B n_e m_{en}(T_e - T_n)}{\lambda_{en}(m_e + m_n)} + \frac{m_n n_e}{\lambda_{en}}\mathbf{u}_{en}\cdot(\mathbf{u}_{en} - \mathbf{u}_n) \\ &\qquad + \frac{3k_B n_i m_{in}(T_i - T_n)}{\lambda_{in}(m_i + m_n)} + \frac{m_n n_i}{\lambda_{in}}\mathbf{u}_{in}\cdot(\mathbf{u}_{in} - \mathbf{u}_n) + R_n\varepsilon_n. \end{aligned} \tag{19}$$

2.4 Numerical implement

For continuous Boltzmann equations, there have been many lattice models to get their discrete forms. In present, $D2Q9$ model is used:

$$e_s^\alpha = \begin{cases} (0,0) & \alpha = 0 \\ \sqrt{3}\left(\cos\left[(\alpha-1)\frac{\pi}{2}\right], \sin\left[(\alpha-1)\frac{\pi}{2}\right]\right)\theta_s & \alpha = 1,2,3,4 \\ \sqrt{6}\left(\cos\left[(2\alpha-1)\frac{\pi}{4}\right], \sin\left[(2\alpha-1)\frac{\pi}{4}\right]\right)\theta_s & \alpha = 5,6,7,8 \end{cases}, \tag{20}$$

where the superscript α denotes the αth component in the phase space and e_s^α is the αth component of the discrete microscopic velocity of particle specie s.

Using the above discrete velocity, the equilibrium distribution functions have related discrete forms:

$$f_s^{\alpha,eq} = \omega^\alpha n_s\left[1 - \frac{\mathbf{e}_s^\alpha\cdot\mathbf{u}_s}{\theta_s^2} + \frac{(\mathbf{e}_s^\alpha\cdot\mathbf{u}_s)^2}{2\theta_s^4} - \frac{\mathbf{u}_s^2}{2\theta_s^2}\right], \tag{21}$$

$$f_{sn}^{\alpha,eq} = \omega^\alpha n_s\left[1 - \frac{\mathbf{e}_s^\alpha\cdot\mathbf{u}_{sn}}{\theta_{sn}^2} + \frac{(\mathbf{e}_s^\alpha\cdot\mathbf{u}_{sn})^2}{2\theta_{sn}^4} - \frac{\mathbf{u}_{sn}^2}{2\theta_{sn}^2}\right], \tag{22}$$

where ω^α has the values

$$\omega^\alpha = \begin{cases} 4/9 & \alpha = 0 \\ 1/9 & \alpha = 1,2,3,4 \\ 1/36 & \alpha = 5,6,7,8 \end{cases}. \tag{23}$$

Finally, the discrete Boltzmann equations can be obtained:

$$\begin{aligned} f_e^\alpha(\mathbf{x} + \mathbf{e}_e^\alpha\Delta t, t + \Delta t) &= f_e^\alpha(\mathbf{x},t) - \frac{f_e^\alpha(\mathbf{x},t) - f_{en}^{\alpha,eq}(\mathbf{x},t)}{\tau_{en}} \\ &\quad + \Delta t\frac{\mathbf{a}_e\cdot(\mathbf{e}_e^\alpha - \mathbf{u}_e)}{\theta_e^2}f_e^{\alpha,eq}(\mathbf{x},t) + \Delta t R_e f_e^{\alpha,eq}(\mathbf{x},t), \end{aligned} \tag{24}$$

$$\begin{aligned} f_i^\alpha(\mathbf{x} + \mathbf{e}_i^\alpha\Delta t, t + \Delta t) &= f_i^\alpha(\mathbf{x},t) - \frac{f_i^\alpha(\mathbf{x},t) - f_{in}^{\alpha,eq}(\mathbf{x},t)}{\tau_{in}} \\ &\quad + \Delta t\frac{\mathbf{a}_i\cdot(\mathbf{e}_i^\alpha - \mathbf{u}_i)}{\theta_i^2}f_i^{\alpha,eq}(\mathbf{x},t) + \Delta t R_i f_i^{\alpha,eq}(\mathbf{x},t), \end{aligned} \tag{25}$$

$$f_n^\alpha(\mathbf{x} + \mathbf{e}_n^\alpha\Delta t, t + \Delta t) = f_n^\alpha(\mathbf{x},t) - \frac{f_n^\alpha(\mathbf{x},t) - f_n^{\alpha,eq}(\mathbf{x},t)}{\tau_{nn}} + \Delta t R_n f_n^{\alpha,eq}(\mathbf{x},t). \tag{26}$$

In eqs. (24)–(26), τ_{sn} is the dimensionless relaxation time of collisions between particle species s and neutrals: $\tau_{sn} = \lambda_{sn}/\Delta t$.

When the above discrete Boltzmann equations are solved, macroscopic parameters of each particle species can be given by

$$n_s(\mathbf{x},t) = \sum_\alpha f_s^\alpha(\mathbf{x},t), \tag{27}$$

$$n_s(\mathbf{x},t)\mathbf{u}_s(\mathbf{x},t) = \sum_\alpha \mathbf{e}_s^\alpha(\mathbf{x},t) f_s^\alpha(\mathbf{x},t). \tag{28}$$

Because plasma has special nature comparing with conventional flow, there are two different procedures when using $D2Q9$ model for plasma. One is a rescaling process implemented before getting the discrete Boltzmann equations,[3] and the other, caused by different species in plasma have significantly different lattice velocities, is an interpolation process is necessary when obtaining on node distribution functions in LBM.[12]

3. Simulation Results

In this paper, two problems are solved to validate the above mathematic models. The first one is the interaction between laser and plasma with temperature change. In this problem, with assumption of 0.01% ionization rate before calculation, inelastic collisions just contain electron impact ionization and three-body recombination. In the second one, there are only neutrals as initial condition, then FDTD and LBM are coupled together for the simulation of multi-photon ionization process of neutrals.

3.1 Interaction between laser and plasma

In this case, 0.01% ionization rate is assumed as an initial condition. It is not necessary to consider the occurrence of initial charged particles. Calculation of change rates of distribution functions by multi-photon ionization is skipped, then total coefficients of ionization and recombination for electrons, ions and neutrals are $R_\mathrm{e} = R_\mathrm{e}^\mathrm{eii} - R_\mathrm{e}^\mathrm{tbr}$, $R_\mathrm{i} = R_\mathrm{e}^\mathrm{eii} n_\mathrm{e}/n_\mathrm{i} - R_\mathrm{e}^\mathrm{tbr} n_\mathrm{e}/n_\mathrm{i}$, and $R_\mathrm{n} = -R_\mathrm{e}^\mathrm{eii} n_\mathrm{e}/n_\mathrm{n} + R_\mathrm{e}^\mathrm{tbr} n_\mathrm{e}/n_\mathrm{n}$, respectively.

Initial parameters of the physical problems are shown in Table I. For simplicity, the continuous laser is simplified as a Gaussian beam. The source of Gaussian beam is set at the bottom line of the computational domain and then laser propagates toward the top. Besides, there is an interface line between laser and plasma perpendicular to laser's propagation direction. In this problem, the coordinate origin is set at the lower left corner of the computational region. The direction of x-axis is from left to right, and y-axis is parallel to laser's propagation direction and directing to the top. At the above coordinate system, the location of the interface line is $y = 47.7\,\mu\mathrm{m}$.

Figure 1 presents electron and ion number densities at 40 ps. Form the figure, we can see electron and ion number densities along laser's propagation centerline are bigger than that in the other region. For a Gaussian beam, intensity of electromagnetic field is Gaussian distributions perpendicular to the beam propagation, so the electrons and ions existing in the centerline of laser can obtained much more laser energy and their kinetic energy increases sharply. Because of electron impact ionization, these electrons with enough kinetic energy can produce new electrons and ions by collisions with neutrals, which is why number densities of charged particles are bigger along laser's centerline. In addition, laser energy is piecemeal absorbed by changed particles when propagating in plasma, the electrons in the upper part of the computational region can be accelerated so slowly that fewer new electrons can be produced in the electron impact ionization process. Therefore, along laser's propagation centerline, number densities of charged particles decrease gradually.

Table I. Parameters about interaction between laser and plasma.

Computational domain (μm^2)	135.68×135.68
Mesh	256×256
Initial electron number density (m^{-3})	2.687×10^{21}
Initial electron temperature (K)	12277.5
Initial ion number density (m^{-3})	2.687×10^{21}
Initial ion temperature (K)	12277.5
Initial neutral number density (m^{-3})	2.687×10^{25}
Initial neutral temperature (K)	12277.5
Laser wavelength (μm)	10.64
Laser intensity ($W \cdot cm^{-2}$)	2×10^8

Notes: because multi-photon ionization is skipped, there are changes in the equations:

(1) Electromagnetic field calculation using FDTD:
eqs. (1) and (2) are used.

(2) Number densities of particles in plasma calculation using LBM:
eqs. (24)–(26) are used, while multi-photon ionization process is skipped, so total coefficients of ionization and recombination in these equations change to $R_\mathrm{e} = R_\mathrm{e}^\mathrm{eii} - R_\mathrm{e}^\mathrm{tbr}$, $R_\mathrm{i} = R_\mathrm{i}^\mathrm{eii} - R_\mathrm{i}^\mathrm{tbr}$, and $R_\mathrm{n} = -R_\mathrm{n}^\mathrm{eii} + R_\mathrm{n}^\mathrm{tbr}$.

(3) Temperature fields calculation using FVM:
eqs. (17)–(19) are used, due to the same reason of the neglected multi-photon ionization process, total coefficients of ionization and recombination change to $R_\mathrm{e} = R_\mathrm{e}^\mathrm{eii} - R_\mathrm{e}^\mathrm{tbr}$, $R_\mathrm{i} = R_\mathrm{i}^\mathrm{eii} - R_\mathrm{i}^\mathrm{tbr}$, and $R_\mathrm{n} = -R_\mathrm{n}^\mathrm{eii} + R_\mathrm{n}^\mathrm{tbr}$.

Temperature fields of electrons and ions at 40 ps are showed in Fig. 2. Along the centerline of laser, temperatures of charged particles are higher, and the reason is similar with that of larger number densities of charged particles. At the same position and time, electron temperature is much higher than that of ions, which is because, in the same electromagnetic field, the heated process of ions with much heavier weight is slower than the process of electrons. Comparing Figs. 2(a) and 2(b), the hot electron area is little larger, which is reasonable because the accelerated process of electrons with lighter weight is faster and then electrons can spread into the broader area within the same time interval than ions.

3.2 Laser induced weakly ionized isothermal helium plasma with multi-photon ionization

In this case, temperature change is neglected in calculation, so in eqs. (9) and (10), $T_\mathrm{en} = T_\mathrm{e}$ and $T_\mathrm{in} = T_\mathrm{i}$ are satisfied. Besides, the calculation processes of eqs. (17)–(19) using FVM are also skipped.

The main purpose of this problem is to validate the applicability of the model to multi-photon ionization, therefore the assumption of three order multi-photon ionization process is used in calculation of the multi-photon ionization cross section.

As the medium of plasma, there are only helium neutrals as the initial condition in the computational domain. The related initial parameters are shown in Table II. For laser, the Gaussian source is also set at the bottom line of the computational domain, but the focusing process is included in FDTD for this problem.

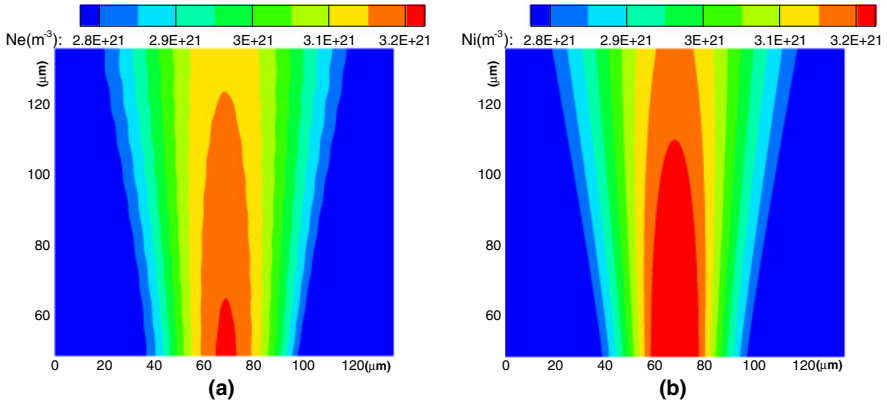

Fig. 1. (Color online) Electron (a) and ion (b) number densities at 40 ps.

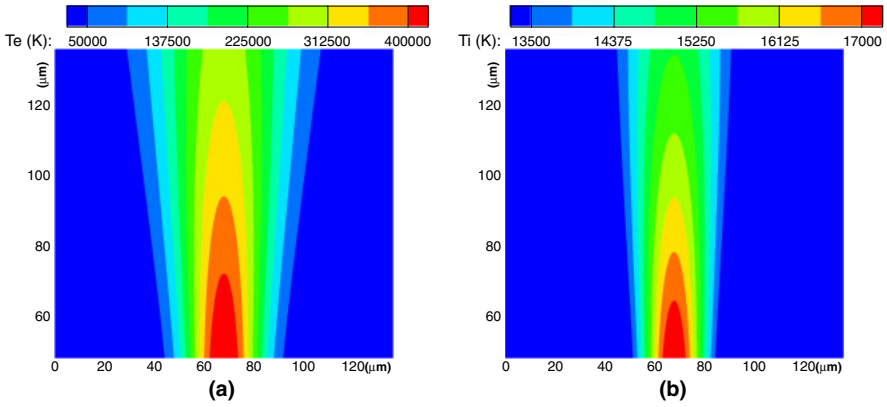

Fig. 2. (Color online) Electron (a) and ion (b) temperature at 40 ps.

Table II. Parameters about laser induced isothermal helium plasma with multi-photon ionization.

Computational domain (μm^2)	135.68×135.68
Mesh	256×256
Initial electron number density (m^{-3})	0
Initial electron temperature (K)	11604.4
Initial ion number density (m^{-3})	0
Initial ion temperature (K)	11604.4
Initial neutral number density (m^{-3})	6.304×10^{23}
Initial neutral temperature (K)	11604.4
Laser wavelength (μm)	10.64
Laser intensity ($W \cdot cm^{-2}$)	5×10^8

Notes: the main calculation processes in this problem:

(1) Electromagnetic field calculation using FDTD: eqs. (1) and (2) are used.

(2) Number densities of particles in plasma calculation using LBM: eqs. (24)–(26) are used, but only isothermal plasma is considered in this problem, so the results of eqs. (9) and (10) can be obtained directly as $T_{en} = T_e$ = electron initial temperature, $T_{in} = T_i$ = ion initial temperature.

(3) Calculation of temperature fields is skipped.

Figure 3 shows number densities of electrons and ions at 5 and 10 ps. From (a) and (b) in Fig. 3, we can see electrons and ions are firstly produced at focus point of laser, which is reasonable because the initial electrons and ions appear mainly depending on multi-photon ionization. The denser photons at laser's focusing point ensure the bigger cross section and then multi-photon ionization process firstly occurs at laser's focus point.

Comparing (a)–(c) and (b)–(d) in Fig. 3, growth of the hot plasma area is obvious. Once initial electrons and ions are produced, they are accelerated and absorb laser energy intensely. After electrons and ions accelerated by the laser, they can move to broader area. Form Fig. 3, we can see that growth of plasma is opposite to laser's propagation direction. This is because the charged particles in the lower area of the computational region firstly come into contact with laser, then they can absorb laser energy more strongly.

In this paper, only single ionization is considered, so the total number of electrons and ions should be equal theoretically. Comparing number densities of electrons and ions at the same position and time, ion number density is much larger than that of electrons. For the same electromagnetic field, the magnitude of Lorentz forces for electrons and ions are equal, while ions with heavier weight can only get smaller accelerator and spread to smaller area comparing with electrons, so ion number density is larger than that of electron at the same position and time.

If the interaction time of laser and plasma is expanded, the growth of plasma becomes slower and slower. In present study, the growth of plasma is mainly depending on multi-photon ionization and electron impact ionization. Once

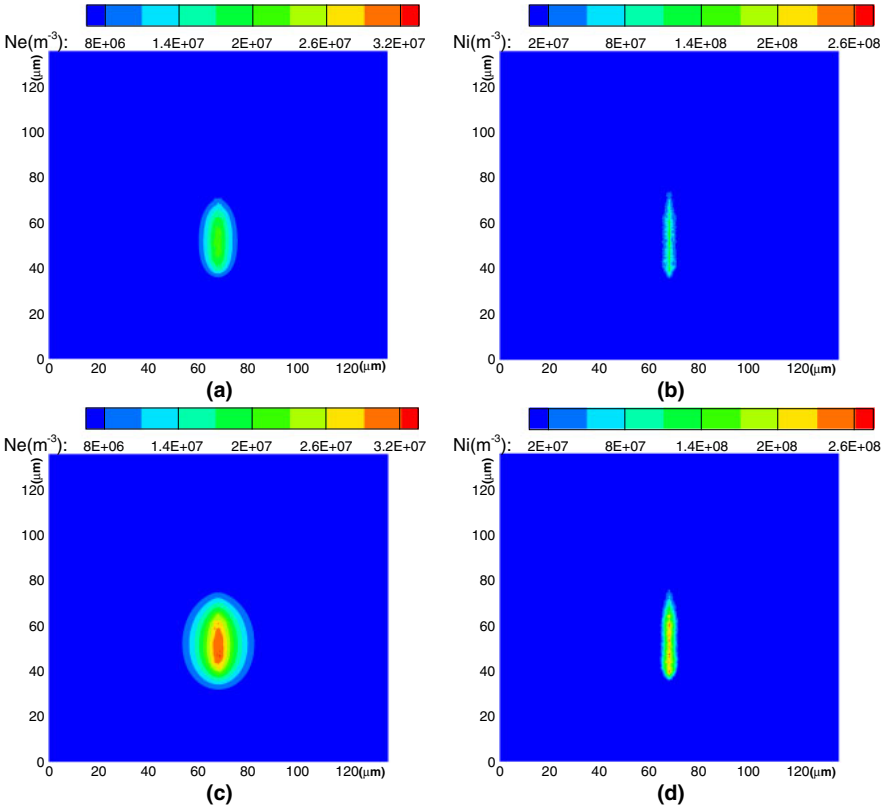

Fig. 3. (Color online) Electron (a, c) and ion (b, d) number densities at 5 (a, b) and 10 (c, d) ps.

initial electrons and ions are produced by multi-photon ionization, they can directly absorb laser's energy by Lorentz force. When electromagnetic energy is obtained by charged particles, the photon number density decreases. The multi-photon ionization rate R_n^{mpi} becomes smaller, so fewer charged particles can be produced by multi-photon ionization. For electron impact ionization, the rate R_e^{eii} increases mainly depending on the cross section and average thermal speed of electrons. These two parameters increase with temperature, while in present study isothermal plasma is assumed, so they cannot obviously increase with the absorbed process of laser energy. Based on the above two reasons, the general result is that plasma's growth becomes slower. In the real generation and development processes of plasma, once electrons are produced by multi-photon ionization, their temperature increases sharply because of acceleration by Lorentz force and frequent collisions with neutrals. The rise of temperature make the number density change coefficient by electron impact ionization increase, so plasma can continue growing.

4. Conclusions

Considering multi-photon ionization, generation of initial charged particles in plasma is simulated by LBM. Charged particles are firstly produced at laser's focusing spot, then accelerated by Lorentz force, they can spread to a broader area. Because of the lighter weight than ions, electrons can expand to a larger area in the same electromagnetic field.

For the interaction between laser and plasma, FDTD, LBM, and FVM are used together for the simulation of weakly ionized helium plasma. Along the centerline of the Gaussian beam, electrons can be accelerated faster and get larger velocities because of the stronger electromagnetic field. Electrons with enough kinetic energy can strengthen electron impact ionization, so number densities of charged particles along the centerline are bigger than other regions. For energy transformation, comparing with electrons, ions are so heavy that their heated process is much slower. This is why temperature of ions is much lower than that of electrons at the same position and time.

1) C. K. Birdsall and A. B. Langdon: *Plasma Physics via Computer Simulation* (Adam Hilger, Bristol, U.K., 1991) p. 218.
2) C. K. Aidun and J. R. Clausen: Annu. Rev. Fluid Mech. **42** (2010) 439.
3) H. Li and Y. Ki: J. Phys. A **42** (2009) 155501.
4) H. Li and Y. Ki: Phys. Rev. E **82** (2010) 016703.
5) A. Taflove and S. C. Hagness: *Computational Electrodynamics: The Finite-Difference Time-Domain Method* (Artech House, Boston, MA, 2000) 3rd ed., p. 308.
6) X. He, X. Shan, and G. D. Doolen: Phys. Rev. E **57** (1998) R13.
7) T. I. Gombosi: *Gaskinetic Theory* (Cambridge University Press, Cambridge, U.K., 1994) pp. 39, 45.
8) N. B. Delone and V. P. Krainov: *Multiphoton Process in Atoms* (Springer, Berlin, 2000) 2nd ed., p. 85.
9) Y. K. Kim and M. E. Rudd: Phys. Rev. A **50** (1994) 3954.
10) A. J. Kemp, R. E. W. Pfund, and J. Meyer-ter-Vehn: Phys. Plasmas **11** (2004) 5648.
11) J. A. Bittencourt: *Fundamentals of Plasma Physics* (Springer, Berlin, 2004) 3rd ed., p. 204.
12) H. Li and Y. Ki: Phys. Rev. E **76** (2007) 066707.